

---

---

# Natural Frequencies of a Viscoelastic Supported Axially Functionally Graded Bar With Tip Masses

**Cihan Demir**

*Department of Mechanical Engineering, Faculty of Mechanical Engineering, Yildiz Technical University, Turkey.*  
Email: cdemir@yildiz.edu.tr

(Received 19 June 2022; accepted 19 November 2022)

The frequency parameters of an Axially Functionally Graded (AFG) bar for viscoelastic and point mass boundary conditions are studied in this paper. The structures with functionally graded materials under axial loads can be modelled as AFG bars. Those may be considered as support elements with spring and dashpot in the vibration isolation. Keeping the ratio of force frequency and natural frequency at a certain level is ensured to control the natural frequency therefore dynamic amplification factor with different material combinations. Various boundary conditions are attained by changing the spring and damping coefficients of viscoelastic support elements and the ratio of rod mass to tip mass. Researchers assume that the beam material properties in directions of length and thickness change exponentially, individually, or both in their studies. There are a few studies on the AFG rods in the existing studies. Analysis is carried out via the finite element method for the non-dimensional frequency parameters of the bar in MATLAB. The energy equations of the motion are obtained in the frame of axial bar theory considering the material properties of the bar vary longitudinally according to the power-law distribution. The effects of material distribution, spring, damping and tip mass values on the bar's frequency parameters and structural behaviour have been extensively investigated.

---

## 1. INTRODUCTION

With the developing technology, the material properties needed in structures are changing. One of the advanced materials that respond to these needs is functionally graded materials that provide unidirectional or bidirectional material exchange. Functionally Graded Material (FGM) can be defined as a particulate composite whose combination is determined by the volume fraction coefficient with the change of more than one material in one or more directions. Structural analysis of plates, bars, beams and shells with FG material has become very important because of their use. Dynamic and static analyses of plates with unidirectional and bidirectional material changes have been carried out by finite element method using different order deformation theories.<sup>1-6</sup> There is less work on the analysis of FG beams and especially bars than on the FG plates and shells. Generally, material properties are considered as varying along the thickness direction in the studies on FGM beams. Also, some of the researchers assumed that the material properties of the beam vary exponentially in both axial and thickness directions called Bi-directional functionally graded materials (BDFGMs). The AFG materials are useful for the static deviation exceeding a certain level or buckling load that a particular purpose. The best functional classification that combines axial direction and thickness is estimated. It can be also considered as a spring element at the supports with different material combinations. The transition from soft to hard material is appropriately provided by the material distribution coefficient "n" in the axial direction. Keeping the ratio of force frequency and natural frequency at a certain level is ensured to control the natural frequency therefore dynamic amplification factor.

In the literature, there are studies on beam structures made of axially functional graded materials in which the material

properties change in the longitudinal and thickness direction. Besides, a modelling approach that includes only longitudinal direction for rods is rare.<sup>15,28</sup>

The following publications can be given as similar in terms of method and boundary conditions for material change throughout the thickness. Sankar<sup>7</sup> investigated the elasticity solution of functional grade beams under harmonic force based on the view of the Euler-Bernoulli beam theory.

Demir and Oz<sup>8</sup> studied the natural frequencies of a FG beam for the viscoelastic supports within the framework of the Euler-Bernoulli beam theory by using the finite element method. The material properties of the beam were considered to vary through thickness according to the power-law distribution. The various stiffness and damping coefficients to viscoelastic support elements were applied to attain different boundary conditions. The effects of various material distribution and boundary conditions were discussed in detail.

Demir and Altinoz<sup>9</sup> studied the harmonic response analysis of a spring supported FG beam within the framework of Timoshenko beam theory by using the finite element method. The effect of the spring values, the material properties and material distribution on the force transmissibility was investigated.

Zenkour and El-Shahrany<sup>10</sup> analyzed the vibrational behavior of a laminated composite beam on Winkler-Pasternak's medium. A higher-order shear deformation theory with an exponential shape function was used to model the proposed system using Hamilton's principle and Navier's approach. The natural frequencies, deflections, and suppression time of the studied system were computed for different thickness ratios, ply orientations, number and location of the magnetostrictive layers, foundation stiffness, velocity feedback gain value, and external force.

Garg et.al.<sup>11</sup> analyzed bending and free vibration analyses of functionally graded carbon nanotube-reinforced (FG-

CNTR) sandwich beams by using the finite element-based higher-order zigzag theory. The effect of different gradation laws which govern the distribution of CNTs across the thickness of face sheets is investigated. The influence of the core's thickness on stresses and displacements is also analyzed. They showed that the thickness of the core and CNT gradation law significantly affect the mechanical behaviour of the sandwich FG-CNTRC beam.

Garg et.al.<sup>12</sup> investigated the bending of sandwich FGM beams under combined hygro-thermo-mechanical loadings considering temperature and moisture-dependent material properties using the finite element-based HOZT. The stress distribution across the thickness of the beam and upward displacement of the sandwich FGM beam was reported.

The articles for AFG beams can be given as follow; the free vibration of an FGM beam on an elastic foundation and spring supports was investigated by Duy et al.<sup>13</sup> The material properties and thickness of the beam were assumed to range in width and length directions obeying the exponential law. An analytical formulation and finite element formulation were used to obtain the natural frequencies of the FGM beams. They showed the effect of spring supports on the natural frequencies of FGM beams.

The response analysis of a simply-supported AFG beam which was loaded harmonically was analyzed in accordance with the theory of Euler–Bernoulli by Simsek et al.<sup>14</sup> The boundary conditions were considered unique spring elements under the combination of thermal and structural effects.

Longitudinal free vibration analysis of AFG microbars was investigated on the basis of strain gradient elasticity theory with comparing with classical theory (CT) for clamped–clamped and clamped-free boundary conditions. The influences of additional material length scale parameters, material ratio, slenderness ratio and the ratio of Young's modulus on natural frequencies of axially FG microbars were shown parametrically by Akgoz.<sup>15</sup> The material properties of microbars were considered to be smoothly varied along the axial direction.

The free vibration of an AFG pile embedded in the Winkler-Pasternak elastic foundation was analyzed within the framework of the Euler-Bernoulli beam theory by Cetin and Simsek.<sup>16</sup> In their study, the material properties of the pile varied continuously in the axial direction according to the power-law form, the effects of material variations and the parameters of the elastic foundation on the fundamental frequencies were examined.

Wadi et. al.<sup>17</sup> calculated the static deflection of axially FG cantilever beam using Rayleigh and Finite Element methods considering Beam Theory of Euler-Bernoulli under the condition of Clamped – Free and Free –Clamped boundary condition. They assumed that the material properties changed along the axial direction of a beam according to the Power-Law Model. The effects of a number of segment, power law index and type of applied load on the dimensionless deflection were studied.

Akgoz and Civalek<sup>18</sup> investigated the vibration behaviour of non-homogenous and non-uniform micro-beams with respect to the Euler-Bernoulli beam and the modified couple stress theory. Material properties and cross-section of the micro-beam were assumed to change in the axial direction of the beam.

They showed the impacts of material properties and conicity ratios on natural frequencies of axially FG tapered microbeams.

The dynamic characteristics of an FG beam with material gradation axially or transversally through the thickness based on the power-law were investigated.<sup>19</sup> The finite element method was employed to discretize the model and obtain a numerical approximation of the motion equation under the assumptions of the Euler–Bernoulli beam theory. They showed the effects of different material distributions, slenderness ratios, and boundary conditions on the dynamic characteristics of the beam.

Huang and Li<sup>20</sup> developed a methodology for free vibration of axially functionally non-uniform graded beams. Aydogdu<sup>21</sup> investigated the AFG simply-supported beam using the semi-inverse method for vibration and buckling.

Ghayesh investigated the mechanics and vibrations of axially functionally graded (AFG) microbeams with the frame of various beam formulations considering linear and nonlinear formulations.<sup>30–33</sup>

The response of the bi-directional functionally graded (BDFG) Timoshenko beam was investigated by Simsek<sup>22</sup> for free and forced vibrations. A moving load was considered an external force. The material properties of the beam varied exponentially in both axial and thickness directions. The formulations of the system were in the frame of Timoshenko beam theory (TBT) and Euler–Bernoulli beam (EBT) theory. The effects of the material distribution, the velocity of moving load, aspect ratio and various boundary conditions on the dynamic responses of the BDFG beam were examined.

Keleshteri and Jelovica<sup>23</sup> analyzed the nonlinear vibration behaviour of shear deformable bidirectional porous beams with non-uniform porosity distribution in the frame of Reddy beam theory considering von Karman geometrical nonlinearity. They proposed a new porosity distribution to maximize the natural frequencies of the porous beam. They showed the effect of geometrical parameters and porosity distributions on the vibration behaviour.

Keleshteri and Jelovica<sup>24</sup> studied the nonlinear free and forced vibration behavior of functionally graded porous beams considering high-order bidirectional porosity distributions. Nonlinear free and forced vibration behavior of bidirectional porous beams under axial loads are investigated based on the Reddy beam Effects of beam's aspect ratio, porosity distributions, beam's shear deformation and porosity volume fraction on the nonlinear free and forced vibration behavior of functionally graded porous beams are studied. It is observed that the method of multiple scales is accurate when the amplitude of vibration and axial load are both small, otherwise, it might significantly underestimate the amplitude of vibration.

Keleshteri and Jelovica<sup>25</sup> reformulated Reddy and Euler–Bernoulli beam theories by using a new function and reduced order of the governing equation in the Generalized differential quadrature (GDQ) method for Buckling and vibration behavior of isotropic, FG and porous beams. Therefore, there is no need extra steps to use for any boundary condition.

The studies for FG beams with point mass can be given as follows; the resonance frequencies were studied for a rotating functional graded clamped beam with point mass by Ramesh and Rao.<sup>26</sup> The materials of the beam consisted of

metal and ceramic. A FG beam with material graduation axially or transversally through the thickness was based on the power-law form. The variation was symmetrically from the core at the midsection to the outer surfaces. The Rayleigh-Ritz method was used to investigate the resonance frequencies of the beam. For modelling the point mass in the system, the Dirac delta function was used. The influence of the material variation, the location and values of a point mass on the resonance frequencies of vibration of the FG beam were investigated. The values of the point mass and its location were found to influence the natural frequencies.

Moukhliss et al.<sup>27</sup> constructed the axial FGM model for a tapered beam. The linear free vibration analysis was performed with discrete mass placement at different points.

In the only study found with the pure axial rod formulation, the FGM modelling was created for a rod in the axial direction and its analysis under a moving heat load was performed by Abouelregal et al.<sup>28</sup>

Studies generally focus on material variation in its thickness or both along the beam and its thickness. Two studies<sup>15,28</sup> of the literature include the modeling only in the axial direction of the AFG structure, for microbeam and, rods under thermal loading. As a contribution to the literature, the effect of the spring, damping and point mass elements at the boundaries and material distribution on the natural frequencies of the bar is examined and their effects on the structural dynamics are investigated. The bar modeled by assuming that the material change of the structure under axial loading changes functionally in the axial direction.

In this paper, an AFG bar is considered as support elements with spring and dashpot for vibration isolation. The functional variation of the material only in the x-axis direction of a bar with the axial load can be assumed as an axial rod. The free vibration of a viscoelastic point supported AFG bar with two-point masses at the ends within the framework of the bar theory is studied. The bar material properties constantly change following the power law in the axial direction. The various values of stiffness and damping are investigated for viscoelastic support. The values of stiffness ( $\kappa$ ) and damping ( $\mu$ ) for the viscoelastic support are taken as zero for free-free boundary conditions.  $\kappa = \infty, \mu = \infty$  values are set providing for clamped boundary condition. The equations governing the motion of the system were developed by the Lagrange method. The results are compared with the exact results of the bar obtained for the particular cases of the problem examined. The effects of various material distributions, the ratio of Young's modulus of right and left ends and boundary conditions are discussed in detail. Tables and graphs are used to represent parametrical results to understand the vibration behaviour of axially graded bars.

## 2. THEORY AND FORMULATIONS

The model consisted of a viscoelastic point supported AFG bar with two masses at the ends. The  $l$  length bar had the physical properties of  $h$  thickness and  $b$  width can be seen in Fig. 1. The subsequent formulations were made with the assumption that deflections occur only in the axial direction and on the x-axis. The Cartesian coordinate system was positioned at the left starting point of the bar, as illustrated in Fig. 1, where  $m_1$ ,

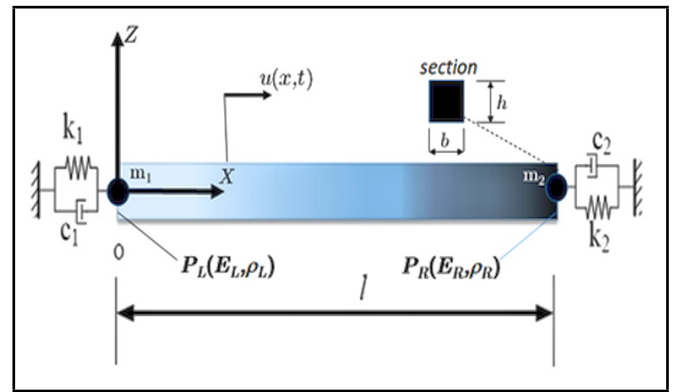


Figure 1. An AFG viscoelastic-supported bar with tip masses.

$m_2$  is point mass at the left and right ends  $k_1, k_2$  are spring coefficients,  $c_1, c_2$  are damping coefficients  $E_L, E_R$  is Young's modulus of left and right surface material, respectively, and  $\rho_L, \rho_R$  are densities of left and right surface material, respectively.

It was assumed that the material properties  $E(x)$ , and  $\rho(x)$  of the FG bar vary longitudinally as a function of the power-law distribution as in Eq. (1) where by taking the exponent  $n$  to be zero, a functional was created such that the material change will be in the material property on the left along the x-axis and with increasing  $n$ , the material on the right will be dominant in the content:

$$P(x) = (P_L - P_R) \left(1 - \frac{x}{L}\right)^n + P_R; \quad (1)$$

where  $P_L$  is material properties of the left surface of the bar,  $P_R$  is material properties of the right surface of the bar, and  $n$  is the power-law exponent.

With this acceptance, the distribution of material and the mechanical properties (elastic modulus and mass density) along the rod depend on the power-law exponent.

The displacement of any point and the unit strain depending on it in the axial direction can be written as in Eq. (2);

$$\varepsilon_{xx} = \frac{\partial u(x, t)}{\partial x} = \frac{\partial u_0(x, t)}{\partial x}. \quad (2)$$

The stresses of the axial bar:

$$\sigma_{xx} = E(x)\varepsilon_{xx}. \quad (3)$$

The strain energy caused by axial deformation of a finite element can be formulated as in Eq. (4):

$$V^{(e)} = \frac{1}{2} \int_0^L \int_A E(x)\varepsilon_{xx}^2 dA dx. \quad (4)$$

Assuming cross-sections constant:

$$A = \int_A dA. \quad (5)$$

The kinetic energy of the AFG bar due to axial displacement is:

$$E_K^{(e)} = \frac{1}{2} \int_V \rho(x)(\dot{u}(x, t))^2 dV; \quad (6)$$

where  $\dot{u}(x, t)$  was the time derivative of the axial displacement of any point on the element.

A two-node finite element of length  $l$  has 1 degree of freedom at each node, 2 totally for the bar model. The nodal displacements for the element are given as follows:

$$\{d^{(e)}\} = [d_i^{(e)}(t), d_j^{(e)}(t)]^T. \quad (7)$$

The axial displacement of any point can be expressed in Eq. (8) by matrix notation:

$$u(x, t) = [N]_x \{d^{(e)}\}^T; \quad (8)$$

where  $[N]_x$  is shape functions for axial displacement.

$$[N]_x = \left\{ 1 - \frac{x}{L} \quad \frac{x}{L} \right\}. \quad (9)$$

$E(x), \rho(x)$  can be rewritten to obey Eq. (1) and substitute into Eq. (4) and Eq. (6), the energy functions can be rewritten for an element as follows in Eq. (10) and Eq. (11):

$$V^{(e)} = \frac{1}{2} A \int_0^L E(x) \left[ ([N']_x \{d\})^2 \right] dx; \quad (10)$$

$$E_k^{(e)} = \frac{1}{2} A \int_0^L \rho(x) \left[ ([N]_x \{\dot{d}\})^2 \right] dx. \quad (11)$$

Eqs. (10) and (11) are rewritten as:

$$V^{(e)} = \frac{1}{2} \left( \{d\}^T A_{xx} A [N']_x^T [N']_x \{d\} \right); \quad (12)$$

$$E_k^{(e)} = \frac{1}{2} \left( \{\dot{d}\}^T \left[ \int_0^L A \rho(x) [N']_x^T [N']_x dx \right] \{\dot{d}\} \right); \quad (13)$$

where:

$$N' = \frac{dN}{dx}; \quad (14)$$

$$A_{xx} = \int_0^L E(x) dx; \quad (15)$$

$$A_{xx} = \frac{(E_L - E_R)L}{n + 1} + E_R L. \quad (16)$$

Terms between generalized displacements and velocity components in strain and kinetic energy expressions include the element stiffness and mass matrices:

$$[K]^e = [A_{xx} A [N']_x^T [N']_x]; \quad (17)$$

$$[M]^e = \left[ \int_0^L \rho(x) A [N']_x^T [N']_x dx \right].$$

The  $2 \times 2$  stiffness and mass matrices for an element:

$$[M]^e = \begin{bmatrix} A \cdot I_A - \frac{2A \cdot I_B}{L} + \frac{A \cdot I_D}{L^2} & \frac{A \cdot I_B}{L} - \frac{A \cdot I_D}{L^2} \\ \frac{A \cdot I_B}{L} - \frac{A \cdot I_D}{L^2} & \frac{A \cdot I_D}{L^2} \end{bmatrix}; \quad (18)$$

$$[K]^e = \begin{bmatrix} \frac{A \cdot A_{xx}}{L^2} & -\frac{A \cdot A_{xx}}{L^2} \\ -\frac{A \cdot A_{xx}}{L^2} & \frac{A \cdot A_{xx}}{L^2} \end{bmatrix};$$

where:

$$I_A = \int_0^L \rho(x) dx = \frac{(\rho_L - \rho_R)L}{n + 1} + \rho_R L; \quad (19)$$

$$I_B = \int_0^L \rho(x) x dx = \frac{(\rho_L - \rho_R)L^2}{(n + 1)(n + 2)} + \rho_R \frac{L^2}{2};$$

$$I_D = \int_0^L \rho(x) x^2 dx = \frac{(\rho_L - \rho_R)L^3}{(n + 1)(n + 2)(n + 3)} + \rho_R \frac{L^3}{3}.$$

To assemble the global system matrices for the finite element model; the kinetic energy of the bar and masses, strain energy of the bar and potential energy of the supports and damping of the supports related to the dissipation function can be expressed in the following form:

$$E_K = \frac{1}{2} \{\dot{d}\}^T [M] \{\dot{d}\} + \frac{1}{2} m_1 \dot{d}_1^2 + \frac{1}{2} m_2 \dot{d}_y^2; \quad (20)$$

$$V = \frac{1}{2} \{d\}^T [K] \{d\}; \quad (21)$$

$$V_s = \frac{1}{2} k_1 d_1^2 + \frac{1}{2} k_2 d_y^2; \quad (22)$$

$$C_S = \frac{1}{2} c_1 \dot{d}_1^2 + \frac{1}{2} c_2 \dot{d}_y^2. \quad (23)$$

Subscript  $y$  represented the global degrees of freedom of the system,  $y = m + 1$ ;  $m$  represented the total element number,  $nn$  represented the total node number of the model;  $nn = m + 1$ ;  $k_1$  and  $k_2$  were the stiffness coefficients of the supports,  $c_1$  and  $c_2$  were the damping coefficients of the supports. The function of the problem for the complete system according to the energy can be written as:

$$F = E_K - (V + V_s). \quad (24)$$

The generalized force for damping  $Q_D$  can be acquired from the dissipation function by differentiating  $C_s$  with respect to  $\dot{d}_h$  where  $h = 1, \dots, y$ :

$$Q_D = -\frac{\partial C_s}{\partial \dot{d}_h}; \quad (25)$$

where  $\dot{d}_h$  is the generalized velocities concerning the nodes. Then, by applying the Lagrange method (Eq. (26)):

$$\frac{\partial F}{\partial d_h} - \frac{d}{dt} \frac{\partial F}{\partial \dot{d}_h} + Q_D = 0; \quad (26)$$

the equations for the complete system are acquired as in Eq. (27):

$$[[K] + [K_s]] \{d\} + [D_s] \{\dot{d}\} [[M_s] + [M]] \{\ddot{d}\} = \{0\}; \quad (27)$$

The rod stiffness was represented by the  $[K]$  matrix, the support stiffness was represented by the  $[K_s]$  matrix, the mass was represented by the  $[M]$  matrix and the damping was represented by the  $D_s$  matrix. The matrices have  $y \times y$  dimensions.  $K_{s11} \neq 0$  and  $K_{sy y} \neq 0$  corresponding to the viscoelastic support values were the only nonzero elements of the  $[K_s]$  matrix.  $D_{s11} \neq 0$  and  $D_{sy y} \neq 0$  corresponding to the viscoelastic support values are the only nonzero elements of the  $[D_s]$  matrix.

The time-dependent changes of the displacements can be represented at the nodal points as in Eq. (28):

$$\{d(t)\} = \{\bar{d}\} e^{i\omega t}. \quad (28)$$

In Eq. (28), the amplitudes  $\{\bar{d}\}$  including the phase angle, were complex variables. In order to investigate the natural frequencies of the viscoelastic supported FG bar, Eq. (28) was substituted for Eq. (27) and can be rewritten in the consequent form:

$$([K] + [K_s] + i\omega[D_s] - \omega^2[[M_s] + [M]]) \{\bar{d}\} = \{0\}. \quad (29)$$

The natural frequency parameters in the dimensionless form are calculated numerically for damped and undamped systems which are supported viscoelastic at the ends. For brevity, the coefficients of  $k_1, k_2$  springs and  $c_1, c_2$  dashpots are taken as having equal values at the two supports denoted by  $k_s$  and  $c_s$  to investigate the resonance frequencies of the FG bar. The values of  $m_1$  and  $m_2$  masses at the ends are also taken as having equal values denoted by  $m_s$ .

### 3. NUMERICAL RESULTS AND DISCUSSION

Numerical results are given in the dimensionless form to make a comparison with the other studies. The non-dimensional spring coefficient  $\kappa$  and the non-dimensional damping coefficient  $\mu$ , the mass ratio  $\beta$  and the non-dimensional resonance frequency  $\lambda$  are the parameters given in Eq. (30):

$$\begin{aligned} \kappa &= \frac{k_s L}{E_L A}; & \mu &= c_s \sqrt{\frac{1}{\rho_L A^2 E_L}}; \\ \beta &= \frac{m_s}{\rho_L A L}; & \lambda^2 &= \frac{\rho_L \omega^2 L^2}{E_L}. \end{aligned} \quad (30)$$

The fundamental frequency equations of the viscoelastic supported bar with tip masses can be rewritten compactly as follows:

$$([K] + \kappa[K_s] + i\mu[D_s] - \lambda^2[[M] + \beta[M_s]]) \{\bar{d}\} = \{0\}. \quad (31)$$

The frequency parameters are calculated from the eigenvalues acquired from the solution of the linear homogeneous equations given in equation Eq. (31) as follows in Eq. (32):

$$\lambda_y = a + ib. \quad (32)$$

#### 3.1. Model Verification

A short investigation is made for the free vibration of a clamped-clamped bar ( $\kappa = \infty$ ) and free-free bar ( $\kappa = 0$ ) by neglecting the effect of damping. The calculated results are compared with the natural frequencies which are obtained from the closed solutions<sup>15,29</sup> for the bar. The value of  $1 \times 10^{100}$  is substituted for the non-dimensional spring coefficient to simulate infinite support stiffness for the clamped boundary condition. The value of 0 is substituted for the non-dimensional spring coefficient  $\kappa$  to simulate zero support stiffness for the free-free boundary condition. Free-free, viscoelastic and clamped-clamped boundary conditions were obtained by varying the dimensionless spring and damping coefficient

**Table 1.** Material properties of components.

	$E$ (GPa)	$\rho$ (kg/m <sup>3</sup> )
Aluminium	70	2700
Alumina (Al <sub>2</sub> O <sub>3</sub> )	380	3800

values between 0 and infinity. By changing the spring and damping values of the viscoelastic support, different boundary conditions are obtained.

The ratio of Young’s modulus can be defined as in Eq. (33):

$$E_{ratio} = \frac{E_R}{E_L}. \quad (33)$$

The ratio of mass densities is taken as in Eq. (34):

$$\rho_{ratio} = \frac{\rho_R}{\rho_L}. \quad (34)$$

The material properties used in the analysis are given in Table 1. The distribution of materials varies continuously from aluminium to alumina, from the left to the right surface.

A homogenous bar condition is obtained when Young’s modulus ratio equals 1. The beam is homogenous when  $E_{ratio} = 1$  and there is no material variation inside the beam, so  $n$  does not have any effect on the frequency parameters. Non-dimensional frequencies of a homogenous bar for the free-free and clamped-clamped boundary conditions are shown in Table 2. The calculated values agree with Rao<sup>29</sup> and Akgoz and Civalek<sup>15</sup> very well.

#### 3.2. The Frequency Parameters of the Bar with the Viscoelastic Boundary Conditions

The frequency parameters of the bar are studied for various values of stiffness and damping parameter. Effects of viscoelastic boundary conditions on the first three frequency parameters are investigated for the non-dimensional spring coefficient  $\kappa = 1, 10, 100, 500, 1000, \infty$  and  $\mu = 0, 1, 3, 10, 200, \infty$ . Table 3, Table 4 and Table 5 show the variation of fundamental non-dimensional frequencies with the different non-dimensional damping coefficient  $\mu$  and power-law exponent  $n$  with the different values of the non-dimensional spring coefficient  $\kappa$ . For the viscoelastic supported bar condition, in the name of investigating the changes of parameters is clearer,  $\beta$  is considered as zero. The evaluations can be written as:

- The frequency parameters increase with increasing  $\mu$  values at the each value of  $\kappa$  for all  $n$  values except the values of  $\kappa = 1$  and  $\mu = 0, 1$  at the first frequency parameter. The variation of the frequency parameters decreases in high values of  $\mu, \kappa$  and the variation is almost zero in some  $\kappa$  and  $\mu$  values (Table 3, Table 4 and Table 5). With the increasing values of  $\kappa$  and  $\mu$ , boundary conditions change from viscoelastic to clamped. As can be seen from Table 3, in the first frequency parameters, at the value of  $\kappa = 1$ ; while  $\mu$  increases from 0 to 1, it is observed that the frequency parameters in all  $n$  values decrease but that decrease doesn’t exist in higher  $\kappa$  values. This is not observed at the second and third frequency parameters. When  $\kappa = 1$  and  $\mu = 0$  at the lower frequency parameter; rigid-body motion is dominant in the

**Table 2.** Non-dimensional frequencies of a free-free and clamped-clamped homogenous bar and the validation studies.

Non-dimensional coefficient	Dimensionless natural frequencies <sup>29</sup>		Dimensionless natural frequencies <sup>15</sup> (Calculated with classical theory, from Table 2)	Present study	
$\lambda^2 = \frac{\rho_L \omega^2 L^2}{E_L}$	$w_{nk} = \frac{k\pi c}{L}, k = 1, 2, \dots$		$E_{ratio} = \frac{E_R}{E_L} = 1$		
	$c = \sqrt{\frac{E}{\rho}}$		$\rho_{ratio} = \frac{\rho_R}{\rho_L} = 1$		
Boundary conditions					
Non-dimensional frequencies	Clamped-Clamped	Free-Free	Clamped-Clamped	Clamped-Clamped	Free-Free
$\lambda_1$	3.14159	3.14159	3.1416	3.14159	3.14159
$\lambda_2$	6.28318	6.28318	6.2832	6.28319	6.28319
$\lambda_3$	9.42477	9.42477	9.4248	9.42498	9.42498

system. When  $\kappa=1$  and  $\mu=1$  at the lower frequency parameter; elastic body motion begins to take effect in the system. This is caused by the transition from a free-free boundary condition ( $\mu = 0$  and  $\kappa = 0$ ) to a clamped boundary condition ( $\mu = \infty$  or  $\kappa = \infty$ ). Between these two regions the system behaves as viscoelastically supported. The rigid-body motion is dominant in the region where  $\kappa = 1$  changes with  $\mu = 0$  and  $\mu = 1$  values while the frequency parameters decrease with increasing  $n$ . Because the density of the bar increases with the increasing  $n$ . While  $n$  increases 0 to 10, the material constituent changes Aluminium to Alumina (Al2O3). The changing values of  $n$  change the material density and also the mass of the bar. While the density of the bar increases the elasticity of the bar decreases in that region. Elastic body motion depends on Young’s modulus ( $E(x)$ ) and the area ( $A$ ) for axial displacement. The material variation coefficient  $n$  is more effective in the elastic body motion. Therefore the increasing  $n$  values, increase the stiffness of the bar and also frequency parameters. In the rigid body motion region,  $n$  is less effective on the variation of the stiffness of the bar.

- The frequency parameters increase with increasing  $\kappa$  values at the values of  $\mu = 0, 1$  for all  $n$  values (Table 3, Table 4 and Table 5). The frequency parameters decrease with increasing  $\kappa$  values up to a minimum frequency value then starts to increase, for all  $n$  values and the values of  $\mu = 3, 10, 200$ . The increasing point of frequency parameter shifts forward with increasing  $\mu$  (Table 3, Table 4 and Table 5). As the spring value of the boundary condition increases, its elastic effect becomes dominant. This effect occurs at different spring values depending on the increasing damping value and the change in natural frequency values occurs accordingly.
- The elastic body motion is dominant in the region where  $\kappa \geq 10$  changes with  $\mu \geq 3$  for the first frequency. The elastic body motion is also dominant for all values of  $\kappa, \mu$  for the second and third frequency parameters. Therefore, the frequency parameters increase with increasing  $n$ . Because of the stiffness increase of bar instead of density increase of bar is dominant in that region.
- When the values of  $\kappa$  and  $\mu$  are 0, the boundary condition corresponds to the free-free state. For this boundary condition, the frequencies correspond to the elastic mode. As the values of  $k$  and  $c$  start to increase from

zero, the boundary conditions change from elastic support to clamped support for both ends. Therefore, for small values of  $\mu$  and  $\kappa$ , rigid modes are effective. For free-free and large values of  $\mu$  and  $\kappa$ , elastic modes are more effective, hence the effect of the material distribution coefficient on the natural frequencies.

### 3.3. The Frequency Parameters of the Bar with the Variations of $E_{ratio}, \kappa$ and $n$

The effect of variations of  $E_{ratio}, \kappa$  and  $n$  on the frequency parameters is investigated for the first three mode frequencies. The ratio of Young’s modulus of the two end materials is examined as a variable. The ratio of mass densities is taken as 1 in line with the general trend in the literature<sup>8,15</sup> to analyze the effect of changing values of Young’s modulus ratio. Figs. 2, 3 and 4 show the variation of the first three non-dimensional frequencies with the different  $E_{ratio}$  and power-law exponent  $n$  with the different values of dimensionless spring values  $\kappa$ . The evaluations can be written as:

- When  $E_{ratio} < 1$ , the frequency parameters corresponding to the  $n = 0$  value remain as an upper limit and the frequency parameters decrease with increasing  $n$  from 0 to 10 (Fig. 2). Decrement of the frequency parameters with the increasing  $n$  increases, while  $E_{ratio}$  decreases from 1 to 0.25 (Fig. 2, Fig. 3, Fig. 4). When  $E_{ratio} > 1$ , the frequency parameters corresponding to the  $n = 0$  value remain as limit inferior and the frequency parameters increase with increasing  $n$  from 0 to 10 (Fig. 2). Increment of the frequency parameters with the increasing  $n$  increases while  $E_{ratio}$  increases from 1 to 10 (Fig. 2, Fig. 3, Fig. 4). The distribution of the material along the bar, the Young’s modulus from big to small or from small to big, the frequency parameters increase or decrease, with the frequency parameter in the homogeneous state of the material being the limit. The left side and right side of the bar have different Young’s modulus and if the ratio of those is greater than 1, the rigidity of the structure increases. Therefore the frequency parameters increase with increasing  $E_{ratio}$ .
- It is observed that the frequency parameters gradually decrease when the springs are considered as support conditions at  $\kappa = 1$  after free-free boundary conditions. While  $\kappa > 1$  the frequency parameters increase with increasing spring constants (Fig. 2, Fig. 3, Fig. 4).



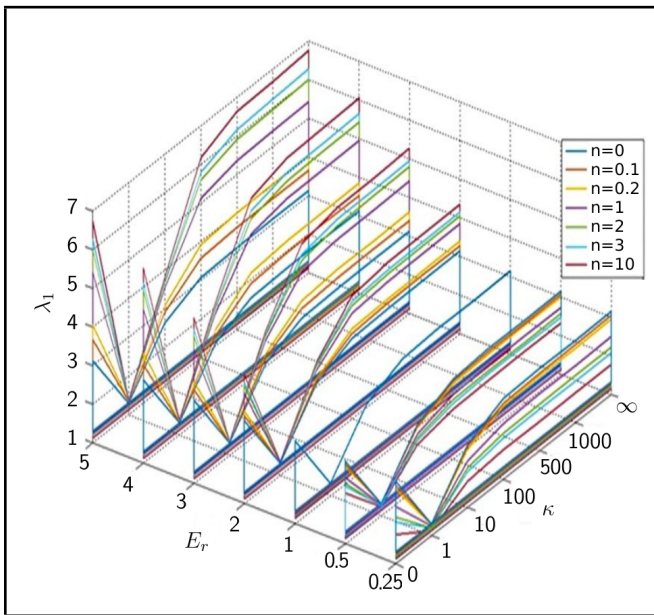


**Figure 2.** 1st frequency parameters for the changes of  $\kappa$  and power-law exponent  $n$  with different values of  $E_{ratio}$ .

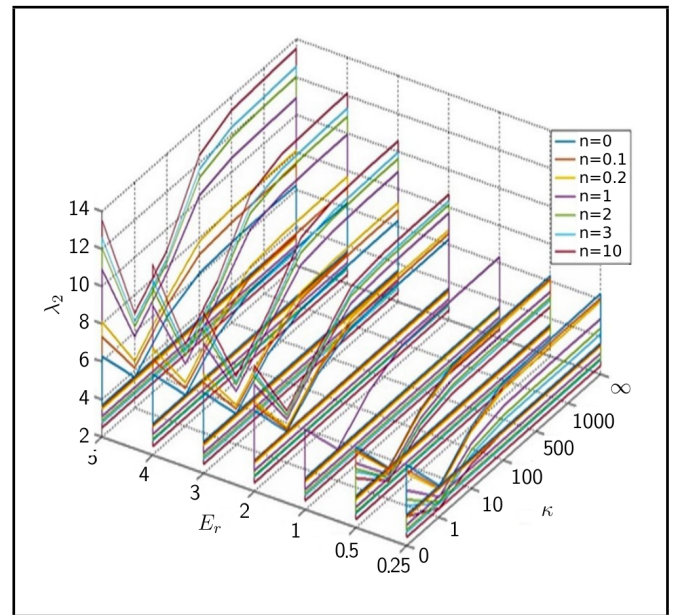


**Figure 3.** 2nd frequency parameters for the changes of  $\kappa$  and power-law exponent  $n$  with different values of  $E_{ratio}$ .

- When  $\kappa$  is zero, the boundary condition is free-free for the bar and the vibration mode of the structure is elastic. When  $\kappa = 1$ , springs join the structure as a boundary condition, the vibration type of the bar is closer to the rigid mode. For the lower spring constants where the rigid body motion is dominant, frequency parameters decrease and the effect of the power-law exponent  $n$  on frequency parameters is little amount because of the rigid body motion of the bar with the springs. The elastic displacements decrease and the effect of the power-law exponent value  $n$  on the frequency parameters also decreases (Fig. 2, Fig. 3, Fig. 4). The elastic-body motion of the bar increases for the second and third frequency parameters. It can be seen from the increasing effect of power-law exponent  $n$  on the frequency parameters (Fig. 2, Fig. 3, Fig. 4).
- After the value of  $\kappa = 500$ , the variation of the frequency parameters depending on parameter  $n$  is a little amount (Fig. 2, Fig. 3, Fig. 4).

### 3.4. The Frequency Parameters of the Bar with the Tip Masses

The effect of tip masses on the first three frequency parameters is studied. The mass ratio  $\beta$  is a variable that is defined as the ratio of bar mass to the point mass. The material properties used in the analysis are given in Table 1. Table 6, Table 7 and Table 8 show the variation of the first three non-dimensional frequencies with the different mass ratio  $\beta$  and power-law exponent  $n$  with the different values of dimensionless spring values  $\kappa$ . The evaluations can be written as:

- The frequency parameters decrease with increasing mass ratio  $\beta$  for each  $\kappa, n$  values. While  $\kappa = 0$  and  $\kappa > 1$  elastic body motion is dominant. Rigid body motion is dominant for  $\kappa = 1$ . The frequency parameters decrease while the values of support increase in the transition from the elastic body motion ( $\kappa = 0$ , free-free boundary condition) to the rigid body motion ( $\kappa = 1$ , viscoelastic support condition). As a result of the increase in mass with increasing

$n$  value, the frequency parameters decrease. As opposed to this, the increasing trend in the frequency parameters is observed in the elastic region with increasing  $\kappa$  spring values and  $n$  power-law exponent values. In the elastic region, it shows that the change in the stiffness of bar due to  $E$  is more effective on the frequency parameter than the change in the mass of bar due to  $n$ . The rigid body motion effect and elastic body motion effect on the frequency parameters is similar to the  $E_{ratio} - \kappa - n$  relation and the effects (Section 3.3). For the  $\kappa$  values where elastic body motion is more dominant and for the free-free boundary conditions, the effects of power-law exponent value  $n$  on the frequency parameters are dominant.

- The mass ratio  $\beta$  effect on the frequency parameters decreases with increasing  $\kappa$  values. Especially, when  $\kappa = \infty$ , for the all  $\beta$  values, frequency parameters converge to the same value. Because of the additional masses act like a support for the higher values of spring constant (Table 6, Table 7 and Table 8).

## 4. CONCLUSION

In this study, AFG bars were concentrated on as a contribution to the limited literature studies. AFG bars can be also considered as support elements like spring and dashpot in the vibration isolation. The functional variation of the material only in the x-axis direction of a bar with the axial load can be assumed as an axial rod. The free vibration of a viscoelastic point-supported AFG bar with tip masses within the framework of the bar theory is studied. The defined dimensionless viscoelastic support values, tip mass values, the ratio of Young's modulus of the two materials and the effects of material distribution on the frequency parameters were examined in detail.

As a result of the evaluations, the following conclusions were obtained:

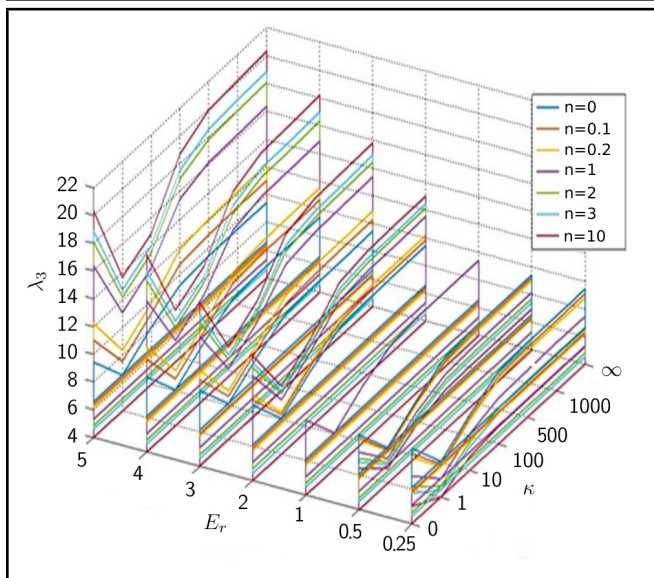


**Figure 4.** 3rd frequency parameters for the changes of  $\kappa$  and power-law exponent  $n$  with different values of  $E_{ratio}$ .

- The frequency parameters increase with the increasing values of  $\kappa$ ,  $\mu$  and  $n$  for the viscoelastic supported FG bar at frequencies where the elastic body motion of the bar and hence its elastic mode is more dominant.
- The power-law exponent  $n$  has a decreasing effect on the first frequencies where the rigid body motion of the bar and hence its rigid mode is more dominant.
- If the AFG rod is added to the system as an isolation element such as a spring, damping element, etc., it should be taken into account that  $n$ , which affects the material distribution, has a different effect on the rigid mode and elastic mode frequencies.
- The values of frequency parameters increase with increasing the values of the ratio of Young's modulus  $E_{ratio}$  and  $\kappa$ . However, the power-law exponent  $n$  has an increasing effect on the frequency parameters when  $E_{ratio} > 1$ , it has a decreasing effect on the frequency parameters when  $E_{ratio} < 1$ . Therefore, which of the young modules on the right and left side is larger will affect the dynamic behavior of the system.
- The frequency parameters decrease with the increasing tip masses. However, increase with increasing the power-law exponent  $n$ . Therefore power-law exponent  $n$  can be used like stiffness  $\kappa$  to control the natural frequency value of the system.
- In general, considering the boundary conditions, as the support values change, the boundary conditions change between free-free, viscoelastic support and fixed support, and the vibration forms also act as rigid body motion, elastic body motion or a combination of them according to increasing spring, damping and tip mass values. The transition from the elastic body motion to the rigid body motion is important for the effect of the material distribution, the values of the coefficients of the viscoelastic support, the ratio of Young's modulus and the tip masses on the frequency parameters. The effects of the material

distribution coefficient  $n$  and the effects of  $E_{ratio}$  on frequency parameters are affected by the transition between elastic-rigid motions.

In future work, variable sectioned FG bar with material damping will be studied using finite element method.

## REFERENCES

- Reddy, J. N., Analysis of functionally graded plates, *Int. J. Numer. Methods Eng.*, **47**(1–3), 663–84, (2000). [https://doi.org/10.1002/\(SICI\)1097-0207\(200011/30\)47:1/3%3C663::AID-NME787%3E3.0.CO;2-8](https://doi.org/10.1002/(SICI)1097-0207(200011/30)47:1/3%3C663::AID-NME787%3E3.0.CO;2-8)
- Zenkour, A. M., Generalized shear deformation theory for bending analysis of functionally graded plates, *Appl. Math. Model.*, **30**(1), 67–84, (2006). <https://doi.org/10.1016/j.apm.2005.03.009>
- Zenkour, A. M., On vibration of functionally graded plates according to a refined trigonometric plate theory, *Int. J. Struct. Stab. Dyn.*, **5**(2), 279–97, (2005). <https://doi.org/10.1142/S0219455405001581>
- Van Do, T., Nguyen, D. K., Duc, N. D., Doan, D. H., Bui, T. Q., Analysis of bi-directional functionally graded plates by FEM and a new third-order shear deformation plate theory, *Thin-Walled Struct.*, **119**, 687–699, (2017). <https://doi.org/10.1016/J.TWS.2017.07.022>
- Vinh, P.V., Formulation of a New Mixed Four-Node Quadrilateral Element for Static Bending Analysis of Variable Thickness Functionally Graded Material Plates, *Math. Probl. Eng.*, 6653350, (2021). <https://doi.org/10.1155/2021/6653350>
- Vinh, P.V., Analysis of bi-directional functionally graded sandwich plates via higher-order shear deformation theory and finite element method, *J. Sandw. Struct. Mater.*, **24**(2):860–899, (2022). <https://doi.org/10.1177/10996362211025811>
- Sankar, B. V., An elasticity solution for functionally graded beams, *Compos. Sci. Technol.*, **61**, 689–696, (2001). [https://doi.org/10.1016/S0266-3538\(01\)00007-0](https://doi.org/10.1016/S0266-3538(01)00007-0)
- Demir, C., Oz, F. E., Free vibration analysis of a functionally graded viscoelastic supported beam, *J. Vib. Control*, **20**(16), 2464–2486, (2014). <https://doi.org/10.1177/1077546313479634>
- Demir, C., Altinoz, M., Vibration analysis of a spring supported fg beam under harmonic force, *Int. J. Acoust. Vib.*, **23**(2), 175–184, (2018). <https://doi.org/10.20855/ijav.2018.23.21358>
- Zenkour, Ashraf M., El-Shahrany, Hela D., Forced Vibration of a magnetoelastic laminated composite beam on pasternak's foundation, *J. Appl. Comput. Mech.*, **52**(3), 478–97, (2021). <https://doi.org/10.22059/jcamech.2021.326538.636>



Table 3. 1st frequency parameters for the changes of  $\mu$  and power-law exponent  $n$  with different values of  $\kappa$ .

$n = 0$						
$\kappa$	$\mu = 0$	$\mu = 1$	$\mu = 3$	$\mu = 10$	$\mu = 200$	$\mu = \infty$
1	1.311393511/	1.214271584	3.060872598	3.135146119	3.141616385	3.14159832
10	2.627679071	2.645888793	2.779244838	3.080438339	3.141462736	3.14159832
100	3.080017867	3.080077427	3.080515098	3.085057322	3.140017409	3.14159832
500	3.129082651	3.129054046	3.129115773	3.129163137	3.136732346	3.14159832
1000	3.135328207	3.135333291	3.135299424	3.13536924	3.137094209	3.14159832
$\infty$	3.14159832	3.14159832	3.14159832	3.14159832	3.14159832	3.14159832
$n = 0.1$						
$\kappa$	$\mu = 0$	$\mu = 1$	$\mu = 3$	$\mu = 10$	$\mu = 200$	$\mu = \infty$
1	1.30654282	1.133749674	3.551986144	3.645778345	3.653600073	3.653591728
10	2.876814389	2.902452697	3.111921751	3.577365702	3.653442649	3.653591728
100	3.553958377	3.554038955	3.555064524	3.564456554	3.65168374	3.653591728
500	3.633209204	3.63327623	3.633193222	3.633334528	3.647054721	3.653591728
1000	3.643372139	3.643357248	3.643416086	3.643409401	3.646889404	3.653591728
$\infty$	3.653591728	3.653591728	3.653591728	3.653591728	3.653591728	3.653591728
$n = 0.2$						
$\kappa$	$\mu = 0$	$\mu = 1$	$\mu = 3$	$\mu = 10$	$\mu = 200$	$\mu = \infty$
1	1.306248341	1.098359973	3.888693871	3.999047793	4.007977114	4.007946587
10	3.013833255	3.043154792	3.307320071	3.920295533	4.007732437	4.007946587
100	3.873423596	3.873641818	3.87499286	3.889594435	4.005815943	4.007946587
500	3.980275495	3.98028978	3.980199796	3.980490632	4.000097599	4.007946587
1000	3.994062869	3.994023891	3.994068414	3.994002276	3.99948349	4.007946587
$\infty$	4.007946587	4.007946587	4.007946587	4.007946587	4.007946587	4.007946587
$n=1$						
$\kappa$	$\mu = 0$	$\mu = 1$	$\mu = 3$	$\mu = 10$	$\mu = 200$	$\mu = \infty$
1	1.256524604	1.028394574	4.917569306	5.120856617	5.133637781	5.133732414
10	3.267015683	3.293871387	3.632403931	5.000722815	5.13342591	5.133732414
100	4.824510375	4.82542833	4.829706616	4.875731257	5.130661323	5.133732414
500	5.068574624	5.068900744	5.068463134	5.069504463	5.121021517	5.133732414
1000	5.100940961	5.10121415	5.100982776	5.101000972	5.117611959	5.133732414
$\infty$	5.133732414	5.133732414	5.133732414	5.133732414	5.133732414	5.133732414
$n=2$						
$\kappa$	$\mu = 0$	$\mu = 1$	$\mu = 3$	$\mu = 10$	$\mu = 200$	$\mu = \infty$
1	1.228281838	1.008480617	5.244514146	5.523891349	5.538444045	5.538651085
10	3.29521361	3.316578677	3.604845822	5.384402671	5.538481527	5.538651085
100	5.134554192	5.135189525	5.141729706	5.206449259	5.535296045	5.538651085
500	5.452468664	5.452185602	5.452694186	5.453624788	5.523622125	5.538651085
1000	5.495215231	5.4951562	5.495284811	5.4950302	5.518780959	5.538651085
$\infty$	5.538651085	5.538651085	5.538651085	5.538651085	5.538651085	5.538651085
$n=3$						
$\kappa$	$\mu = 0$	$\mu = 1$	$\mu = 3$	$\mu = 10$	$\mu = 200$	$\mu = \infty$
1	1.214337726	0.999720594	5.363599012	5.700027991	5.715592033	5.715664482
10	3.297802499	3.316352277	3.569509416	5.551046586	5.715220928	5.715664482
100	5.263126176	5.263936648	5.27159016	5.345711639	5.711796379	5.715664482
500	5.618566917	5.61882712	5.618434522	5.619847118	5.69966917	5.715664482
1000	5.666705339	5.666273289	5.666366098	5.666625101	5.693918111	5.715664482
$\infty$	5.715664482	5.715664482	5.715664482	5.715664482	5.715664482	5.715664482
$n=10$						
$\kappa$	$\mu = 0$	$\mu = 1$	$\mu = 3$	$\mu = 10$	$\mu = 200$	$\mu = \infty$
1	1.188413882	0.984430132	5.465021267	5.999174034	6.016604273	6.016472435
10	3.28901954	3.302653064	3.485607203	5.830975995	6.015923065	6.016472435
100	5.470339521	5.471249901	5.481005262	5.57441465	6.012554594	6.016472435
500	5.897937952	5.897970555	5.897758373	5.899604384	5.998466142	6.016472435
1000	5.956613385	5.956883241	5.956230401	5.956358109	5.991433574	6.016472435
$\infty$	6.016472435	6.016472435	6.016472435	6.016472435	6.016472435	6.016472435

Table 4. 2nd frequency parameters for the changes of  $\mu$  and power-law exponent  $n$  with different values of  $\kappa$ .

$n = 0$						
$\kappa$	$\mu = 0$	$\mu = 1$	$\mu = 3$	$\mu = 10$	$\mu = 200$	$\mu = \infty$
1	3.673204337	4.331729065	6.243273705	6.279993053	6.283306898	6.283190918
10	5.307354733	5.420839949	5.959298398	6.251508877	6.283124645	6.283190918
100	6.160184824	6.160618489	6.163962295	6.192899623	6.282442508	6.283190918
500	6.258203108	6.258181268	6.258265871	6.258619364	6.27975463	6.283190918
1000	6.270693588	6.270643506	6.270696803	6.270772304	6.278388397	6.283190918
$\infty$	6.283190918	6.283190918	6.283190918	6.283190918	6.283190918	6.283190918
$n = 0.1$						
$\kappa$	$\mu = 0$	$\mu = 1$	$\mu = 3$	$\mu = 10$	$\mu = 200$	$\mu = \infty$
1	4.115970356	4.406616597	7.256333141	7.303440017	7.307358108	7.307189941
10	5.873647888	6.021746337	6.863580215	7.268448736	7.307163071	7.307189941
100	7.108303724	7.109113754	7.116362106	7.172618365	7.30626261	7.307189941
500	7.26646373	7.266634706	7.266469241	7.267371593	7.302963546	7.307189941
1000	7.286787228	7.286714885	7.286737998	7.286929678	7.300640948	7.307189941
$\infty$	7.307189941	7.307189941	7.307189941	7.307189941	7.307189941	7.307189941
$n = 0.2$						
$\kappa$	$\mu = 0$	$\mu = 1$	$\mu = 3$	$\mu = 10$	$\mu = 200$	$\mu = \infty$
1	4.427171943	4.609834997	7.955311468	8.011535822	8.01577199	8.015930176
10	6.221844029	6.3827339	7.468103059	7.9718037	8.015808194	8.015930176
100	7.747608556	7.74899887	7.759829029	7.844161423	8.014923742	8.015930176
500	7.960603361	7.960644132	7.96066812	7.961845643	8.011034299	8.015930176
1000	7.98817293	7.988315461	7.988064433	7.988179445	8.00820833	8.015930176
$\infty$	8.015930176	8.015930176	8.015930176	8.015930176	8.015930176	8.015930176
$n=1$						
$\kappa$	$\mu = 0$	$\mu = 1$	$\mu = 3$	$\mu = 10$	$\mu = 200$	$\mu = \infty$
1	5.438373023	5.491253255	10.14944035	10.26135209	10.26765408	10.26751709
10	7.153150026	7.291199523	9.115191965	10.20188618	10.26749985	10.26751709
100	9.654184467	9.658797356	9.692883714	9.933452862	10.26574416	10.26751709
500	10.13724528	10.13754085	10.13743207	10.14244963	10.26053221	10.26751709
1000	10.20194823	10.20216957	10.2017582	10.20262162	10.25505409	10.26751709
$\infty$	10.26751709	10.26751709	10.26751709	10.26751709	10.26751709	10.26751709
$n=2$						
$\kappa$	$\mu = 0$	$\mu = 1$	$\mu = 3$	$\mu = 10$	$\mu = 200$	$\mu = \infty$
1	5.8088865	5.843860982	10.9060705	11.06980046	11.07715921	11.07733154
10	7.442493274	7.558770926	9.452875627	11.0020565	11.07718659	11.07733154
100	10.27878396	10.28487497	10.3316646	10.66319447	11.07562609	11.07733154
500	10.90510022	10.90467998	10.90594246	10.91248896	11.06913839	11.07733154
1000	10.99050908	10.99046414	10.99045997	10.99103119	11.06214823	11.07733154
$\infty$	11.07733154	11.07733154	11.07733154	11.07733154	11.07733154	11.07733154
$n=3$						
$\kappa$	$\mu = 0$	$\mu = 1$	$\mu = 3$	$\mu = 10$	$\mu = 200$	$\mu = \infty$
1	5.971771914	6.000610732	11.21849949	11.42338849	11.43106732	11.43145752
10	7.563799549	7.669919253	9.509071198	11.35109614	11.43152422	11.43145752
100	10.5388666	10.54620545	10.59958966	10.97667746	11.42962938	11.43145752
500	11.23733506	11.23809968	11.23802654	11.24636431	11.4220467	11.43145752
1000	11.33346796	11.33292099	11.33359931	11.33456042	11.414899	11.43145752
$\infty$	11.43145752	11.43145752	11.43145752	11.43145752	11.43145752	11.43145752
$n=10$						
$\kappa$	$\mu = 0$	$\mu = 1$	$\mu = 3$	$\mu = 10$	$\mu = 200$	$\mu = \infty$
1	6.24963095	6.270756821	11.66785839	12.02421696	12.03251145	12.03302002
10	7.764009786	7.853777485	9.449924965	11.94266096	12.03280078	12.03302002
100	10.96014416	10.9686625	11.0346196	11.5017187	12.03093117	12.03302002
500	11.7961667	11.79576953	11.7974906	11.80792712	12.02284048	12.03302002
1000	11.91329759	11.91351955	11.91394462	11.91507224	12.01484799	12.03302002
$\infty$	12.03302002	12.03302002	12.03302002	12.03302002	12.03302002	12.03302002

Table 5. 3rd frequency parameters for the changes of  $\mu$  and power-law exponent  $n$  with different values of  $\kappa$ .

$n = 0$						
$\kappa$	$\mu = 0$	$\mu = 1$	$\mu = 3$	$\mu = 10$	$\mu = 200$	$\mu = \infty$
1	6.584679102	7.563824642	9.398467371	9.422830058	9.424940831	9.424987793
10	8.067240786	8.33663695	9.18195677	9.403667987	9.424869417	9.424987793
100	9.24064611	9.242044501	9.25303207	9.32398838	9.424420413	9.424987793
500	9.387399194	9.387449326	9.387522604	9.388547463	9.422502496	9.424987793
1000	9.406133333	9.406120937	9.406108877	9.406280083	9.420860112	9.424987793
$\infty$	9.424987793	9.424987793	9.424987793	9.424987793	9.424987793	9.424987793
$n = 0.1$						
$\kappa$	$\mu = 0$	$\mu = 1$	$\mu = 3$	$\mu = 10$	$\mu = 200$	$\mu = \infty$
1	7.561268278	7.888508318	10.92681909	10.95840256	10.96092569	10.96099854
10	9.034421459	9.349507824	10.6400847	10.93520904	10.96099719	10.96099854
100	10.6634406	10.66644457	10.68893253	10.81875575	10.9603172	10.96099854
500	10.89980892	10.89991719	10.90029685	10.90262701	10.95793535	10.96099854
1000	10.93028826	10.93036615	10.93038698	10.93067438	10.95571835	10.96099854
$\infty$	10.96099854	10.96099854	10.96099854	10.96099854	10.96099854	10.96099854
$n = 0.2$						
$\kappa$	$\mu = 0$	$\mu = 1$	$\mu = 3$	$\mu = 10$	$\mu = 200$	$\mu = \infty$
1	8.242554587	8.428666227	11.98357586	12.02099473	12.02408327	12.02398682
10	9.672368639	9.987102737	11.63515685	11.99459551	12.02389127	12.02398682
100	11.62329404	11.62806321	11.6618191	11.84888759	12.02335153	12.02398682
500	11.94103599	11.94075039	11.94114858	11.94557903	12.02071605	12.02398682
1000	11.98237743	11.98251879	11.98253891	11.98293486	12.01798953	12.02398682
$\infty$	12.02398682	12.02398682	12.02398682	12.02398682	12.02398682	12.02398682
$n = 1$						
$\kappa$	$\mu = 0$	$\mu = 1$	$\mu = 3$	$\mu = 10$	$\mu = 200$	$\mu = \infty$
1	10.42674843	10.47291267	15.32115857	15.39788948	15.40143464	15.40142822
10	11.61590863	11.8217715	14.6023762	15.35730796	15.40144347	15.40142822
100	14.49374525	14.5082118	14.60901327	15.09251094	15.40018171	15.40142822
500	15.20614079	15.20643825	15.20763186	15.22253273	15.3968395	15.40142822
1000	15.30308814	15.3035153	15.30348742	15.3051694	15.39207787	15.40142822
$\infty$	15.40142822	15.40142822	15.40142822	15.40142822	15.40142822	15.40142822
$n = 2$						
$\kappa$	$\mu = 0$	$\mu = 1$	$\mu = 3$	$\mu = 10$	$\mu = 200$	$\mu = \infty$
1	11.21750374	11.24711672	16.49939682	16.61135106	16.6163602	16.61627197
10	12.30369167	12.46224884	15.46071604	16.56639308	16.61623661	16.61627197
100	15.44112031	15.4600565	15.59644789	16.24358284	16.61511467	16.61627197
500	16.3580304	16.35684889	16.3601376	16.38161472	16.61091664	16.61627197
1000	16.48596013	16.48569993	16.48673584	16.48830021	16.60592853	16.61627197
$\infty$	16.61627197	16.61627197	16.61627197	16.61627197	16.61627197	16.61627197
$n = 3$						
$\kappa$	$\mu = 0$	$\mu = 1$	$\mu = 3$	$\mu = 10$	$\mu = 200$	$\mu = \infty$
1	11.56381225	11.5876303	17.00115619	17.14216434	17.14667931	17.14727783
10	12.60435209	12.74470445	15.73724542	17.09431159	17.14713426	17.14727783
100	15.8379632	15.85856902	16.01330949	16.74273695	17.14644868	17.14727783
500	16.85649504	16.85735509	16.85820869	16.88535822	17.14041366	17.14727783
1000	17.00003218	16.99900482	17.00040543	17.00430392	17.13518204	17.14727783
$\infty$	17.14727783	17.14727783	17.14727783	17.14727783	17.14727783	17.14727783
$n = 10$						
$\kappa$	$\mu = 0$	$\mu = 1$	$\mu = 3$	$\mu = 10$	$\mu = 200$	$\mu = \infty$
1	12.15320879	12.1709236	17.79502807	18.04454291	18.048597	18.04974365
10	13.115915	13.22775158	15.93927217	17.98937192	18.05035985	18.04974365
100	16.4857437	16.51059158	16.69477066	17.58612958	18.04783376	18.04974365
500	17.69497401	17.69500189	17.69872629	17.7318039	18.04358428	18.04974365
1000	17.86989193	17.87054867	17.87077387	17.87520828	18.0361361	18.04974365
$\infty$	18.04974365	18.04974365	18.04974365	18.04974365	18.04974365	18.04974365

Table 6. 1st dimensionless frequencies with different  $\beta$  and power-law exponent  $n$  with different values of  $\kappa$ .

$n=0$							
$\kappa$	$\beta=0$	$\beta=0.25$	$\beta=0.75$	$\beta=1$	$\beta=3$	$\beta=5$	$\beta=10$
0	3.1415987	2.1537492	1.4720110	1.3065431	0.7944963	0.6221056	0.4435213
1	1.3113939	1.1119371	0.8821077	0.8086748	0.5335924	0.4261034	0.3085481
10	2.6276796	2.5503343	2.3666566	2.2678728	1.6536241	1.3374055	0.9738771
100	3.0800172	3.0785539	3.0754182	3.0737352	3.0567049	3.0297197	2.8451265
500	3.1290834	3.1290208	3.1288972	3.1288332	3.1283052	3.1277315	3.1260576
1000	3.1353288	3.1353120	3.1352815	3.1352663	3.1351381	3.1350053	3.1346468
$\infty$	3.1415987	3.1415987	3.1415987	3.1415987	3.1415987	3.1415987	3.1415987
$n = 0.1$							
$\kappa$	$\beta=0$	$\beta=0.25$	$\beta=0.75$	$\beta=1$	$\beta=3$	$\beta=5$	$\beta=10$
0	3.6535921	2.5300981	1.7371080	1.5430650	0.9399980	0.7363222	0.5251070
1	1.3065431	1.1098650	0.8788545	0.8057436	0.5324144	0.4254594	0.3082903
10	2.8768144	2.7504106	2.4774644	2.3464662	1.6599611	1.3381624	0.9735353
100	3.5539583	3.5508104	3.5439211	3.5401445	3.4987154	3.4226060	2.9694643
500	3.6332094	3.6330751	3.6328004	3.6326601	3.6314684	3.6301347	3.6259920
1000	3.6433717	3.6433382	3.6432695	3.6432344	3.6429491	3.6426485	3.6418138
$\infty$	3.6535921	3.6535921	3.6535921	3.6535921	3.6535921	3.6535921	3.6535921
$n = 0.2$							
$\kappa$	$\beta=0$	$\beta=0.25$	$\beta=0.75$	$\beta=1$	$\beta=3$	$\beta=5$	$\beta=10$
0	4.0079469	2.7977464	1.9280199	1.7137743	1.0455324	0.8192567	0.5843965
1	1.3062486	1.1043199	0.8750688	0.8026277	0.5313585	0.4248994	0.3080705
10	3.0138338	2.8507539	2.5231920	2.3763185	1.6609544	1.3376299	0.9730577
100	3.8734239	3.8683870	3.8571977	3.8509691	3.7787691	3.6371355	3.0026628
500	3.9802751	3.9800554	3.9796068	3.9793764	3.9773958	3.9751253	3.9676897
1000	3.9940630	3.9940080	3.9938951	3.9938387	3.9933672	3.9928651	3.9914430
$\infty$	4.0079469	4.0079469	4.0079469	4.0079469	4.0079469	4.0079469	4.0079469
$n=1$							
$\kappa$	$\beta=0$	$\beta=0.25$	$\beta=0.75$	$\beta=1$	$\beta=3$	$\beta=5$	$\beta=10$
0	5.1337312	3.6978304	2.5883653	2.3072404	1.4166643	1.1116411	0.7938295
1	1.2565248	1.0694749	0.8556108	0.7871904	0.5265260	0.4223802	0.3070955
10	3.2670152	3.0037538	2.5679201	2.3976320	1.6531648	1.3318498	0.9703630
100	4.8245088	4.8068666	4.7659914	4.7422960	4.4434770	3.9730821	3.0336214
500	5.0685732	5.0677370	5.0659990	5.0650972	5.0569429	5.0466920	5.0048509
1000	5.1009416	5.1007280	5.1002931	5.1000703	5.0981874	5.0960832	5.0895769
$\infty$	5.1337312	5.1337312	5.1337312	5.1337312	5.1337312	5.1337312	5.1337312
$n=2$							
$\kappa$	$\beta=0$	$\beta=0.25$	$\beta=0.75$	$\beta=1$	$\beta=3$	$\beta=5$	$\beta=10$
0	5.5386522	4.0446184	2.8520509	2.5457780	1.5680818	1.2313234	0.8797746
1	1.2282823	1.0509874	0.8456743	0.7793581	0.5241045	0.4211198	0.3066072
10	3.2952119	3.0096101	2.5588121	2.3871782	1.6470049	1.3283022	0.9688982
100	5.1345537	5.1087679	5.0484544	5.0132555	4.5831606	4.0130144	3.0345964
500	5.4524675	5.4511888	5.4485185	5.4471223	5.4342683	5.4174730	5.3420976
1000	5.4952150	5.4948869	5.4942171	5.4938737	5.4909334	5.4875871	5.4768144
$\infty$	5.5386522	5.5386522	5.5386522	5.5386522	5.5386522	5.5386522	5.5386522
$n=3$							
$\kappa$	$\beta=0$	$\beta=0.25$	$\beta=0.75$	$\beta=1$	$\beta=3$	$\beta=5$	$\beta=10$
0	5.7156648	4.2008531	2.9728548	2.6554063	1.6381776	1.2868181	0.9196748
1	1.2143373	1.0418794	0.8407671	0.7754869	0.5229005	0.4204912	0.3063631
10	3.2978014	3.0053331	2.5515169	2.3801729	1.6437379	1.3264742	0.9681566
100	5.2631258	5.2329942	5.1623384	5.1210680	4.6290132	4.0236742	3.0341173
500	5.6185670	5.6170381	5.6138368	5.6121599	5.5965776	5.5758653	5.4789964
1000	5.6666917	5.6662981	5.6654939	5.6650819	5.6615312	5.6574571	5.6440889
$\infty$	5.7156648	5.7156648	5.7156648	5.7156648	5.7156648	5.7156648	5.7156648
$n=10$							
$\kappa$	$\beta=0$	$\beta=0.25$	$\beta=0.75$	$\beta=1$	$\beta=3$	$\beta=5$	$\beta=10$
0	6.0164720	4.4735033	3.1869630	2.8502840	1.7636415	1.3862993	0.9912874
1	1.1884111	1.0248888	0.8315569	0.7682039	0.5206194	0.4192979	0.3058992
10	3.2890199	2.9890657	2.5346910	2.3649446	1.6373186	1.3229326	0.9667314
100	5.4703264	5.4316011	5.3406419	5.2876115	4.6884721	4.0347139	3.0321962
500	5.8979372	5.8958849	5.8915666	5.8892946	5.8678621	5.8385179	5.6921419
1000	5.9566011	5.9560716	5.9549821	5.9544237	5.9495683	5.9439134	5.9247209
$\infty$	6.0164720	6.0164720	6.0164720	6.0164720	6.0164720	6.0164720	6.0164720

Table 7. 2nd dimensionless frequencies with different  $\beta$  and power-law exponent  $n$  with different values of  $\kappa$ .

$n = 0$							
$\kappa$	$\beta = 0$	$\beta = 0.25$	$\beta = 0.75$	$\beta = 1$	$\beta = 3$	$\beta = 5$	$\beta = 10$
0	6.2832351	4.5778665	3.8141887	3.6732020	3.3405115	3.2639955	3.2041592
1	3.6732043	2.6130838	1.7997816	1.5985137	0.9731483	0.7619493	0.5432052
10	5.3073547	4.6791954	3.5244612	3.1581357	1.9431357	1.5230123	1.0862559
100	6.1601848	6.1476674	6.1144194	6.0901997	5.4016621	4.3988574	3.1617733
500	6.2582031	6.2577045	6.2566488	6.2560857	6.2505398	6.2423289	6.1640510
1000	6.2706936	6.2705697	6.2703126	6.2701812	6.2697571	6.2673439	6.2626278
$\infty$	6.2831909	6.2831909	6.2831909	6.2831909	6.2831909	6.2831909	6.2831909
$n = 0.1$							
$\kappa$	$\beta = 0$	$\beta = 0.25$	$\beta = 0.75$	$\beta = 1$	$\beta = 3$	$\beta = 5$	$\beta = 10$
0	7.3072279	5.3584640	4.4830230	4.2909038	3.8927190	3.8009985	3.7287971
1	4.1159704	2.9263592	2.0203713	1.7956632	1.0949749	0.8576336	0.6115919
10	5.8736479	4.9724041	3.6520020	3.2654750	2.0060922	1.5725484	1.1218053
100	7.1083037	7.0808200	6.9986906	6.9355397	5.5411461	4.4305070	3.1748916
500	7.2664637	7.2653657	7.2629748	7.2616921	7.2488739	7.2224416	6.7535116
1000	7.2867872	7.2865044	7.2859457	7.2855998	7.2829406	7.2821307	7.2640619
$\infty$	7.3071899	7.3071899	7.3071899	7.3071899	7.3071899	7.3071899	7.3071899
$n = 0.2$							
$\kappa$	$\beta = 0$	$\beta = 0.25$	$\beta = 0.75$	$\beta = 1$	$\beta = 3$	$\beta = 5$	$\beta = 10$
0	8.0159407	5.9088194	4.9117814	4.7243217	4.2778074	4.1742650	4.0928492
1	4.4271719	3.1564687	2.1852661	1.9433249	1.1866627	0.9297263	0.6631604
10	6.2218440	5.1501413	3.7461841	3.3477194	2.0566984	1.6125490	1.1505511
100	7.7476086	7.7030742	7.5606056	7.4968980	5.6065469	4.4484429	3.1851215
500	7.9606034	7.9587851	7.9548314	7.9526578	7.9274953	7.8661143	6.9028091
1000	7.9881729	7.9877046	7.9867761	7.9864272	7.9807053	7.9757423	7.9396031
$\infty$	8.0159302	8.0159302	8.0159302	8.0159302	8.0159302	8.0159302	8.0159302
$n = 1$							
$\kappa$	$\beta = 0$	$\beta = 0.25$	$\beta = 0.75$	$\beta = 1$	$\beta = 3$	$\beta = 5$	$\beta = 10$
0	10.2675248	7.7295998	6.4040773	6.1460402	5.5201139	5.3726152	5.2559847
1	5.4383730	3.9606550	2.7802669	2.4858360	1.5233534	1.1951220	0.8606147
10	7.1531500	5.6873509	4.1038732	3.6698866	2.2636697	1.7768091	1.2765289
100	9.6541845	9.4924831	8.8691426	8.4955734	5.7148879	4.5102813	3.2358768
500	10.1372453	10.1302274	10.1139578	10.0993612	9.9331410	9.0299554	7.0805006
1000	10.2019482	10.2001597	10.1964006	10.1942720	10.1750297	10.1333631	9.6156248
$\infty$	10.2675171	10.2675171	10.2675171	10.2675171	10.2675171	10.2675171	10.2675171
$n = 2$							
$\kappa$	$\beta = 0$	$\beta = 0.25$	$\beta = 0.75$	$\beta = 1$	$\beta = 3$	$\beta = 5$	$\beta = 10$
0	11.0773705	8.4191389	6.9675982	6.6803085	5.9772061	5.8102134	5.6778021
1	5.8088865	4.2793500	3.0250091	2.7090586	1.6649288	1.3070729	0.9422234
10	7.4424933	5.8909835	4.2614329	3.8145269	2.3592281	1.8529569	1.3327935
100	10.2787840	10.0457852	9.2370716	8.6937195	5.7510152	4.5379712	3.2577570
500	10.9051002	10.8936907	10.8716793	10.8461708	10.4273806	9.3625039	7.0781304
1000	10.9905091	10.9877723	10.9808769	10.9833234	10.9425031	10.8621849	9.8595881
$\infty$	11.0773315	11.0773315	11.0773315	11.0773315	11.0773315	11.0773315	11.0773315
$n = 3$							
$\kappa$	$\beta = 0$	$\beta = 0.25$	$\beta = 0.75$	$\beta = 1$	$\beta = 3$	$\beta = 5$	$\beta = 10$
0	11.4313995	8.7286515	7.2198347	6.9189567	6.1793620	6.0030176	5.8629984
1	5.9717719	4.4240762	3.1380810	2.8125932	1.7310362	1.3594281	0.9804735
10	7.5637995	5.9836981	4.3363687	3.8874287	2.4053185	1.8897576	1.3597407
100	10.5388666	10.2461455	9.3483685	8.6950839	5.7678290	4.5515101	3.2690208
500	11.2373351	11.2244562	11.1880697	11.1772565	10.5143573	9.4796325	7.0811896
1000	11.3334680	11.3302037	11.3229681	11.3192404	11.2739997	11.1586482	9.9031954
$\infty$	11.4314575	11.4314575	11.4314575	11.4314575	11.4314575	11.4314575	11.4314575
$n = 10$							
$\kappa$	$\beta = 0$	$\beta = 0.25$	$\beta = 0.75$	$\beta = 1$	$\beta = 3$	$\beta = 5$	$\beta = 10$
0	12.0330176	9.2690011	7.6581008	7.3970304	6.5773052	6.3331868	6.1790528
1	6.2496310	4.6780924	3.3397009	2.9978988	1.8501043	1.4538652	1.0496221
10	7.7640098	6.1474914	4.4731411	4.0160303	2.4904978	1.9854685	1.4104647
100	10.9601442	10.6133678	9.5071464	9.0211661	5.7984771	4.5768949	3.2897792
500	11.7961667	11.7775901	11.7361787	11.7188210	10.8198305	9.5920208	7.0858051
1000	11.9132976	11.9083168	11.8992884	11.8935527	11.8272679	11.6041047	10.0081207
$\infty$	12.0330200	12.0330200	12.0330200	12.0330200	12.0330200	12.0330200	12.0330200



Table 8. 3rd dimensionless frequencies with different  $\beta$  and power-law exponent  $n$  with different values of  $\kappa$ .

$n = 0$							
$\kappa$	$\beta = 0$	$\beta = 0.25$	$\beta = 0.75$	$\beta = 1$	$\beta = 3$	$\beta = 5$	$\beta = 10$
0	9.4249457	7.2872558	6.6774136	6.5846723	6.3875124	6.3462446	6.3172316
1	6.5846791	4.7390061	3.8655990	3.7076924	3.3462335	3.2662443	3.2046025
10	8.0672408	6.3041906	4.5345947	4.1695490	3.4455661	3.2956892	3.2111043
100	9.2406461	9.1921138	8.9782326	8.7105524	5.8135190	4.5965189	3.4741809
500	9.3873992	9.3856766	9.3817107	9.3794117	9.3461107	9.1778585	7.0509063
1000	9.4061333	9.4057080	9.4047143	9.4043102	9.3993357	9.3915065	9.2542176
$\infty$	9.4249878	9.4249878	9.4249878	9.4249878	9.4249878	9.4249878	9.4249878
$n = 0.1$							
$\kappa$	$\beta = 0$	$\beta = 0.25$	$\beta = 0.75$	$\beta = 1$	$\beta = 3$	$\beta = 5$	$\beta = 10$
0	10.9609491	8.5071099	7.7812569	7.6724700	7.4324305	7.3832074	7.3454196
1	7.5612683	5.4943734	4.5027778	4.3206464	3.8979582	3.8029824	3.7293306
10	9.0344215	6.8377050	5.0335588	4.6842813	3.9733445	3.8268027	3.7348619
100	10.6634406	10.5547097	9.9814997	9.3121030	5.9160630	4.7301547	3.9542418
500	10.8998089	10.8959724	10.8866801	10.8809935	10.7511144	9.7417224	7.0771322
1000	10.9302883	10.9293243	10.9272720	10.9261537	10.9128455	10.8860129	9.8668243
$\infty$	10.9609985	10.9609985	10.9609985	10.9609985	10.9609985	10.9609985	10.9609985
$n = 0.2$							
$\kappa$	$\beta = 0$	$\beta = 0.25$	$\beta = 0.75$	$\beta = 1$	$\beta = 3$	$\beta = 5$	$\beta = 10$
0	12.0240282	9.3611004	8.5500970	8.4250099	8.1578403	8.1017233	8.0590711
1	8.2425546	6.0311339	4.9520551	4.7516000	4.2824680	4.1761147	4.0933481
10	9.6723686	7.2394094	5.4212433	5.1147046	4.3467968	4.1972150	4.0983977
100	11.6232940	11.4406962	10.3671878	9.5455119	6.0349577	4.8873296	4.2281046
500	11.9410360	11.9347102	11.9187754	11.9099159	11.5739487	9.8751597	7.0967716
1000	11.9823774	11.9808333	11.9773710	11.9754262	11.9523797	11.8779231	9.9354188
$\infty$	12.0239868	12.0239868	12.0239868	12.0239868	12.0239868	12.0239868	12.0239868
$n = 1$							
$\kappa$	$\beta = 0$	$\beta = 0.25$	$\beta = 0.75$	$\beta = 1$	$\beta = 3$	$\beta = 5$	$\beta = 10$
0	15.4014389	12.1461655	11.0304418	10.8534794	10.4719028	10.3911985	10.3297514
1	10.4267484	7.8210803	6.4360451	6.1680420	5.5240631	5.3742040	5.2530904
10	11.6159086	8.7010258	6.7713364	6.3275690	5.5675699	5.3902274	5.2167151
100	14.4937452	13.8306459	11.1789360	10.0621271	6.6818526	5.7483653	5.1557225
500	15.2061408	15.1812129	15.0960166	15.0489267	12.6106775	10.0157568	7.0805008
1000	15.3030881	15.2968934	15.2820513	15.2734750	15.0778251	13.6921264	10.0030414
$\infty$	15.4014282	15.4014282	15.4014282	15.4014282	15.4014282	15.4014282	15.4014282
$n = 2$							
$\kappa$	$\beta = 0$	$\beta = 0.25$	$\beta = 0.75$	$\beta = 1$	$\beta = 3$	$\beta = 5$	$\beta = 10$
0	16.6162233	13.1835101	11.9421774	11.7425498	11.3100182	11.2182249	11.1482676
1	11.2175037	8.5020954	6.9974646	6.7010189	5.9810081	5.8117523	5.6753663
10	12.3036917	9.2896999	7.1591577	6.8846376	6.0206307	5.8268375	5.6384332
100	15.4411203	14.4948158	11.4078457	10.2667824	6.8296519	6.2806410	5.5702245
500	16.3580304	16.3191321	16.1971428	16.0922591	12.7232963	10.0663194	7.0781307
1000	16.4859601	16.4765174	16.4532338	16.4282647	15.8385204	13.8976981	10.0058765
$\infty$	16.6162720	16.6162720	16.6162720	16.6162720	16.6162720	16.6162720	16.6162720
$n = 3$							
$\kappa$	$\beta = 0$	$\beta = 0.25$	$\beta = 0.75$	$\beta = 1$	$\beta = 3$	$\beta = 5$	$\beta = 10$
0	17.1472741	13.6447276	12.3451770	12.1347588	11.6688797	11.5805828	11.5065029
1	11.5638122	8.8073037	7.2488777	6.9391678	6.1831133	6.0045406	5.8607306
10	12.6043521	9.5587972	7.4402261	7.2740781	6.2214578	6.0193212	5.8237463
100	15.8379632	14.7659254	11.5120118	10.3655351	6.9748833	6.4193955	5.7518484
500	16.8564950	16.8094121	16.6591915	16.5242355	12.7595601	10.0920059	7.0811899
1000	17.0000322	16.9891796	16.9611083	16.9402771	16.2910422	13.9413354	10.0072923
$\infty$	17.1472778	17.1472778	17.1472778	17.1472778	17.1472778	17.1472778	17.1472778
$n = 10$							
$\kappa$	$\beta = 0$	$\beta = 0.25$	$\beta = 0.75$	$\beta = 1$	$\beta = 3$	$\beta = 5$	$\beta = 10$
0	18.0497104	14.4403553	13.0373079	12.9100361	12.3047556	12.1977350	12.1159703
1	12.1532088	9.3376283	7.6858501	7.3523130	6.5304833	6.3346904	6.1770293
10	13.1159150	10.1205238	7.9304311	7.6268959	6.5671320	6.2448683	6.1402240
100	16.4857437	15.1666063	11.7009603	10.5495735	7.3028555	6.7346839	6.0612035
500	17.6949740	17.6152650	17.4133092	17.2139022	12.8192099	10.1417398	7.0858053
1000	17.8698919	17.8549023	17.8140980	17.7885512	16.8897657	13.9959143	10.0100574
$\infty$	18.0497437	18.0497437	18.0497437	18.0497437	18.0497437	18.0497437	18.0497437

- <sup>11</sup> Garg, A., Chalak, H. D., Zenkour, A. M., Belarbi, M. O., Sahoo, R., Bending and free vibration analysis of symmetric and unsymmetric functionally graded CNT reinforced sandwich beams containing softcore, *Thin-Walled Struct.*, **170**, 108626, (2022). <https://doi.org/10.1016/J.TWS.2021.108626>
- <sup>12</sup> Aman, G., Chalak, H. D., Belarbi, Mohamed-Ouejdi, Zenkour, A. M., Hygro-thermo-mechanical based bending analysis of symmetric and unsymmetric power-law, exponential and sigmoidal FG sandwich beams, *Mech. Adv. Mater. Struct.*, **29**(25), 4523–454, (2021). <https://doi.org/10.1080/15376494.2021.1931993>
- <sup>13</sup> Duy, H.T., Van, T.N., Noh, H.C., Eigen analysis of functionally graded beams with variable cross-section resting on elastic supports and elastic foundation, *Struct. Eng. Mech.*, **52**(5), 1033–1049, (2014). <https://doi.org/10.12989/sem.2014.52.5.1033>
- <sup>14</sup> Simsek, M., Kocaturk, T., Akbas, S.D., Dynamic behavior of an axially functionally graded beam under action of a moving harmonic load, *Compos. Struct.*, **94**(8), 2358–2364, (2012). <https://doi.org/10.1016/j.compstruct.2012.03.020>
- <sup>15</sup> Akgoz, B., Civalek, O., Longitudinal vibration analysis of strain gradient bars made of functionally graded materials (FGM). *Compos. B. Eng.*, **55**, 263–268, (2013). <https://doi.org/10.1016/j.compositesb.2013.06.035>
- <sup>16</sup> Cetin, D., Simsek, M., Free vibration of axially functionally graded pile with pinned ends embedded in Winkler-Pasternak elastic medium, *Struct. Eng. Mech.*, (2011). <https://doi.org/10.12989/sem.2011.40.4.583>
- <sup>17</sup> Wadi, K. J., Yadeem, J. M., Khazaal, M., S., Al-Ansari, L. S., Abdulsamad, H. J., Static deflection calculation for axially FG cantilever beam under uniformly distributed and transverse tip loads. *Results Eng.*, **14**, 100395, (2022). <https://doi.org/10.1016/J.RINENG.2022.100395>
- <sup>18</sup> Akgoz, B., Civalek, O., Free vibration analysis of axially functionally graded tapered Bernoulli–Euler microbeams based on the modified couple stress theory, *Compos. Struct.*, **98**, 314–322, (2013). <https://doi.org/10.1016/j.compstruct.2012.11.020>
- <sup>19</sup> Alshorbagy, A.E., Eltaher, M.A., Mahmoud, F.F., Free vibration characteristics of a functionally graded beam by finite element method, *Appl. Math. Model.*, **35**(1), 412–425, (2011). <https://doi.org/10.1016/j.apm.2010.07.006>
- <sup>20</sup> Huang, Y., Li, X.F., A new approach for free vibration of axially functionally graded beams with non-uniform cross-section, *J. Sound Vib.*, **329**(11), 2291–2303, (2010). <https://doi.org/10.1016/j.jsv.2009.12.029>
- <sup>21</sup> Aydogdu, M., Semi-inverse method for vibration and buckling of axially functionally graded beams, *J. Reinf. Plast. Compos.*, **27**(7), 683–691, (2008). <https://doi.org/10.1177%2F0731684407081369>
- <sup>22</sup> Simsek, M., Bi-directional functionally graded materials (BDFGMs) for free and forced vibration of Timoshenko beams with various boundary conditions, *Compos. Struct.*, **133**, 968–978, (2015). <https://doi.org/10.1016/j.compstruct.2015.08.021>
- <sup>23</sup> Keleshteri, M. M., Jelovica, J., Analytical assessment of nonlinear forced vibration of functionally graded porous higher order hinged beams, *Compos. Struct.*, **298**, 115994, (2022). <https://doi.org/10.1016/J.COMPSTRUCT.2022.115994>
- <sup>24</sup> Keleshteri, M.M., Jelovica, J., Nonlinear vibration analysis of bidirectional porous beams, *Eng. Comput.*, (2021). <https://doi.org/10.1007/s00366-021-01553-x>
- <sup>25</sup> Keleshteri, M. M., Jelovica, J., Beam theory reformulation to implement various boundary conditions for generalized differential quadrature method, *Eng. Struct.*, **252**, 113666, (2022). <https://doi.org/10.1016/J.ENGSTRUCT.2021.113666>
- <sup>26</sup> Ramesh, M.N.V., Rao, N. M., Chordwise bending vibration analysis of functionally graded beams with concentrated mass, *Procedia Eng.*, **64**, 1374–1383, (2013). <https://doi.org/10.1016/j.proeng.2013.09.219>
- <sup>27</sup> Moukhliiss, A., Rahmouni, A., Bouksour, O., Benamar, R., Using the discrete model for the processing of natural vibrations, tapered beams made of AFG materials carrying masses at different spots, *Mater. Today Proc.*, **52**(1), 22–28, (2022). <https://doi.org/10.1016/J.MATPR.2021.10.107>
- <sup>28</sup> Abouelregal, A.E., Yao, S.W., Ahmad, H., Analysis of a functionally graded thermopiezoelectric finite rod excited by a moving heat source, *Results Phys.*, **19**, 103389, (2020). <https://doi.org/10.1016/J.RINP.2020.103389>
- <sup>29</sup> Rao, S. S., *Mechanical Vibrations*, 5th edn. Prentice Hall, New Jersey (2010).
- <sup>30</sup> Ghayesh, M. H., Nonlinear oscillations of FG cantilevers, *Applied Acoustics*, **145**, 393–398. (2019). <https://doi.org/10.1016/J.APACOUST.2018.08.014>
- <sup>31</sup> Ghayesh, M. H., Nonlinear Vibrations of Axially Functionally Graded Timoshenko Tapered Beams, *ASME. J. Comput. Nonlinear Dynam.*, **13**(4), 041002, (2018). <https://doi.org/10.1115/1.4039191>
- <sup>32</sup> Ghayesh, M.H., Mechanics of tapered AFG shear-deformable microbeams, *Microsyst Technol*, **24**, 1743–1754, (2018). <https://doi.org/10.1007/s00542-018-3764-y>
- <sup>33</sup> Ghayesh, M. H., Vibration analysis of shear-deformable AFG imperfect beams, *Compos. Struct.*, **200**, 910–920, (2018). <https://doi.org/10.1016/J.COMPSTRUCT.2018.03.091>